JOURNAL OF Materials CHEMISTRY
Feature Article

Materials in nanoporous alumina

Günter Schmid

Institut für Anorganische Chemie, University of Essen, Germany.
E-mail: guenter.schmid@uni-essen.de

Received 23rd November 2001, Accepted 25th January 2002
First published as an Advance Article on the web 21st March 2002

Nanoporous alumina membranes are easily available by controlled anodization of aluminium surfaces in aqueous acids. Their properties, such as optical transparency, temperature stability, and pores of variable widths and lengths, make them a unique material to be filled by optically or magnetically interesting elements and compounds on the nanoscale. Magnetic nanowires of Fe, Co, and Ni are formed by AC deposition from aqueous solutions. Gold colloids were generated inside the pores by growing smaller particles or by using preprepared particles. Siloxenes, gallium nitride, and cadmium sulfide have been made inside the pores from appropriate precursors resulting in photoluminescent alumina membranes.

Introduction

Nanoporous alumina is a unique material in several respects. It can easily be prepared in any size and shape by anodic oxidation of aluminium surfaces in polyprotic aqueous media. It is optically transparent, temperature stable up to 1000 °C and, above all, the diameter of the parallel running pores can easily be varied from *ca.* 5 nm up to 300 nm. In addition, the pore length simply depends on the anodization time. The material 'alumina' is not identical with crystalline Al_2O_3, but is composed of amorphous oxide-hydrates with inclusions of ions of the acid used for anodization. On the other hand, it can be transformed to more or less well defined γ-Al_2O_3 by annealing at appropriate temperatures. Freshly prepared and simply dried alumina membranes exhibit, owing to their OH-covered inner and outer surfaces, considerable chemical activity that can be used for manifold modifications. The pores in alumina membranes therefore offer a tremendous number of applications as nanotubes in which nanosized materials can be fabricated or filled in. Furthermore, appropriate modifications of the pore walls by functionalized molecules opens unlimited possibilities to ionically or covalently bind other species inside these transparent alumina windows.

This article deals with the use of nanoporous alumina to generate metallic nanowires, nanoparticles of metals and semiconductors, and of photoluminescent materials.

Nanoporous alumina membranes

The formation of oxide layers on aluminium is a well known process. It happens in air by itself, but can also be promoted by chemical or electrochemical processes. Self-oxidation of aluminium is usually a welcome process as it protects this less noble metal from further corrosion. Artificial oxidation is used if the oxide surface needs to be equipped with distinct properties, such as a porous structure. Anodization is the most successful technique to reach a nanoporous surface. Technically fabricated materials of aluminium are often covered with an artificial nanoporous oxide layer to absorb various colors for decoration. For most purposes described in this feature article, however, free-standing membranes without an aluminium support are required in order to benefit from the transparency or the membrane function in the case of drug delivery.

The mechanism of the anodization process is meanwhile quite well understood and described in the literature.[1–5] In a first step a so-called barrier layer, which is a closed thin oxide layer on the aluminium surface, is formed when an aluminium plate is used as the anode. Lead and other metals can serve as cathodes. The barrier layer is characterized by numerous defects, originally caused by defects in the aluminium surface. Owing to the decreasing current with the increase of the thickness of the barrier layer the formation of pores is initiated at defect positions. Supported by the electric field, aluminium oxide and hydroxide at the pore walls are preferentially dissolved by the acidic electrolyte which may consist of diluted sulfuric acid, phosphoric acid or oxalic acid. When the electric field increases by increasing the voltage the dissolution process is accelerated, *i.e.* larger pores are formed. Roughly it was found that a voltage of 1 V causes a pore growth of 1.2 nm. Moderate temperatures of +10–0 °C improve the quality of the pores. Under special conditions even hexagonally ordered pore patterns can be generated. Fig. 1 shows some details of membrane formation. Fig. 2[6] shows a transmission electron microscopic (TEM) image of a cutout of a thin membrane surface with *ca.* 50 nm pores. The TEM image in Fig. 3[7] gives an insight into the inner pore structure of a membrane.

To remove a membrane from the aluminium support the oxidized plate can be dipped into dilute hydrochloric acid to dissolve part of the aluminium. The evolving hydrogen gas then

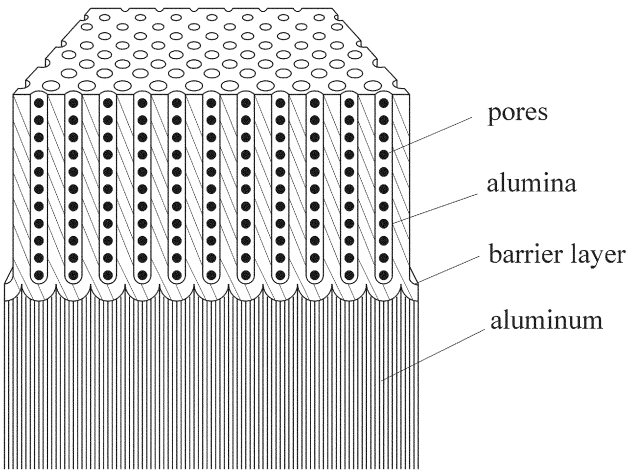

Fig. 1 Sketch of an alumina membrane on aluminium filled with nanoparticles including the barrier layer.

DOI: 10.1039/b110753b

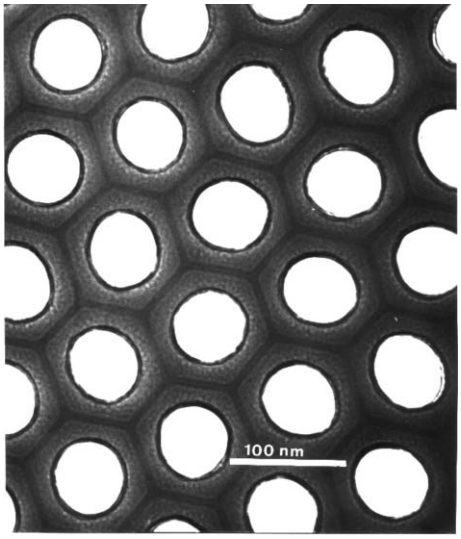

Fig. 2 Transmission electron microscopy (TEM) image of a thin alumina membrane ion milled showing hexagonally ordered, *ca.* 50 nm pores.[6]

Fig. 3 TEM image of a nanoporous alumina membrane with *ca.* 60 nm pores, sectioned perpendicular to the surface showing parallel pores.[7]

removes the membrane layer from the metal. If thin aluminium foils are used for oxidation, the remaining metal can also be removed by bromine which does not attack the oxide layer. In both cases flexible alumina membranes are yielded which are then washed and dried in air or at elevated temperatures to become glass-like, fragile windows. They still bear the barrier layer at the back side. If this has to be removed, the membrane can be chemically etched in an alcoholic KOH bath. Membranes with open pores on both sides result.

Metal nanowires in the pores

The generation of metallic nanowires is of considerable interest for magnetic metals. Fundamental questions arise with respect to the relation of the geometric dimensions of a wire and its magnetic behavior. Furthermore, materials like alumina membranes, filled with magnetic wires could be considered as promising future candidates for storage devices, bearing in mind that the membranes offer between 10^9 and 10^{11} pores per cm^2.

In principle there exist two general methods to deposit metals in nanopores: chemical[8–12] and electrical deposition.[9,13–21] The electrical deposition can be performed under DC or AC conditions. Since this chapter will deal exclusively with magnetic metal wires generated by AC deposition, only this method shall be briefly described.

Aluminium plates which had been anodized on only one side were used as an electrode. The 10–20 nm thick barrier layer between the metal and the porous layer is of special relevance with respect to the AC filling process. It acts as a rectifier that preferentially conducts the cathodic current (valve oxide). During the anodic half-cycles, deposited metal is dissolved again. The length of the nanowires depends directly on the plating time. Fe, Co, and Ni were deposited from aqueous sulfate solutions. The aluminium layer can be removed by chemical etching with bromine or phosphoric acid. Fig. 4 shows a TEM image of a sectioned membrane filled with Ni nanowires. It turned out that the pores are either completely filled or empty, and thus giving bundles of magnetically active wires which run parallel through the membrane but which are separated from each other. Occasional defects have no effect on the overall membrane structure.[22]

These composites are ideal systems particularly to study the anisotropic magnetic nature of the wires. In the case of iron, Mössbauer spectroscopy is another tool used to obtain information on the nature of the wires. It was found that most parts of the Fe nanowires consist of metallic α-Fe. Small amounts of Fe(III) could also be detected, probably caused by partial oxidation at the pore ends. However, it was also found

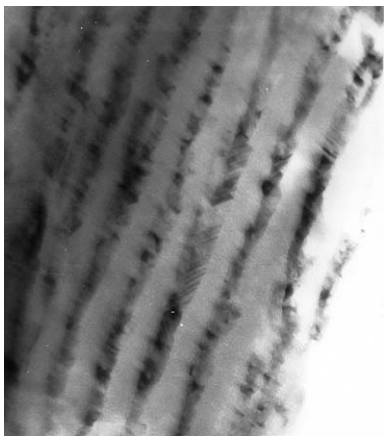

Fig. 4 TEM image of a sectioned alumina membrane filled with electrolytically deposited nickel wires. Pore width *ca.* 25 nm.[22]

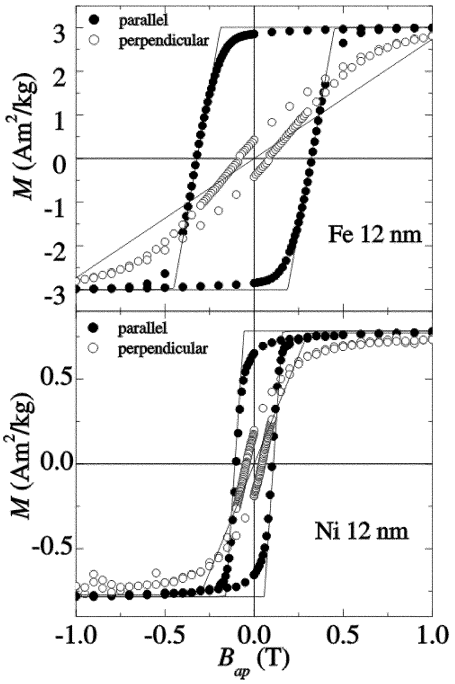

Fig. 5 Hysteresis loops of 12 nm Fe and Ni wires at 4.7 K. Solid lines indicate numerical calculations of the time-dependent magnetization.[22]

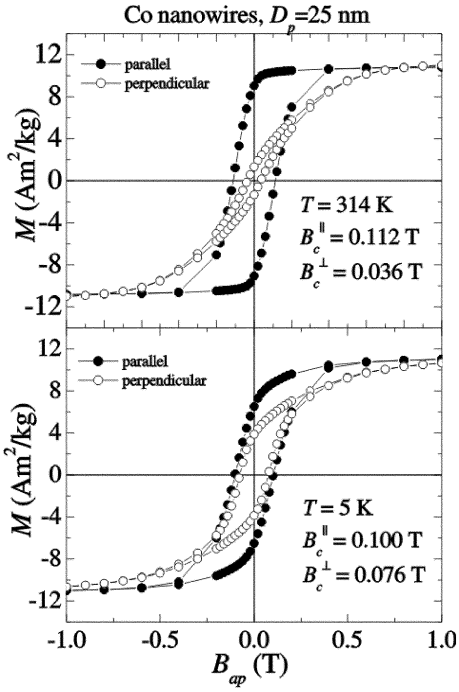

Fig. 6 Hysteresis loops of 25 nm Co wires at 314 and 5 K.[22]

that no further oxidation takes place even over long periods of time in air.

The shape anisotropy of an individual wire causes two stable orientations of the magnetic moment: parallel and perpendicular to the wire axis. Fig. 5 shows the hysteresis loops of 12 nm Fe and Ni wires.

Theoretically, the hysteresis loop has a rectangular shape.[23,24] With magnetic fields applied parallel to the wire axis the hysteresis loop is indeed almost square. Perpendicularly applied fields, however, cause loops that are more or less closed, as expected. Weak interactions between the wires lead to small shearing of the loops.

The magnetic anisotropy of Co wires differs characteristically from that of Fe and Ni. Whereas for Fe- and Ni-filled pores the geometric anisotropy dominates, the geometric and the magneto crystalline anisotropy constants for hexagonal cobalt are almost identical. This is why we can expect two competing mechanisms. Of decisive importance is the orientation of the crystallographic *c* axis, which corresponds in hexagonal cobalt with the slight magnetization, in relation to the long axis of the pore. If the *c* axis lies parallel to the long pore axis, both effects may intensify each other. If they are perpendicularly oriented, however, a mutual weakening can be expected. Fig. 6 shows the hysteresis loops of Co wires of 25 nm in diameter at two different temperatures.

At 314 K, the curve is reminiscent of the hysteresis loops of Fe and Ni, indicating that the easy axes of magnetization lie mainly along the long pore axis, whereas measurement perpendicular to the long axis is almost free of hysteresis. This represents the clear dominance of the geometric anisotropy. At 5 K, however, the magnetization curve changes, especially for perpendicularly applied fields. The easy axis is no longer fully parallel to the pore axis. Furthermore, the hysteresis of the measurements perpendicular to the long axis is much more pronounced. This is attributed to the different temperature dependences of the anisotropy constants.

Optical properties of gold nanoparticles

Optical properties of nanosized metal particles have been studied intensively during the past decades, both experimentally and theoretically.[25] Mathematical descriptions have allowed a deeper understanding of intrinsic and of extrinsic properties. Above all, the famous Mie theory must be mentioned in this connection.[26] It was found that not only are the kind of metal and the particle size of relevance for the optical properties, but also the surrounding medium as well as particle interactions. Nanoporous alumina membranes are very well suited for the study of optical properties, not only for their transparency, but likewise for their variable pore structure which can be used for one-dimensional particle arrangements.

To generate wire-like structures of gold nanoparticles two approaches have been used:[27] the thermal decomposition of smaller particles in the pores to create larger colloids, and the transport of preformed particles into the pores (vacuum induction). As easily degradable small particles, $Au_{55}(PPh_3)_{12}Cl_6$ clusters were used. Decomposition temperatures from 100 to 800 °C have been applied. As it turned out, there is no relation between pore diameter and the resulting particle size for decomposition temperatures up to 400–500 °C. The particles are all between 4 and 5 nm in diameter. Above 500 °C, larger particles up 10–11 nm are formed, due to coalescence processes. We attribute this effect to the thermal behavior of small metal particles in good qualitative agreement with the thermodynamic model of Reifenberger and coworkers.[28] Some extinction spectra of such gold–alumina nanocomposites are shown in Fig. 7.

Two absorption peaks can be observed. The low energy plasmon resonances are due to absorption along the long axis of wire-like structures of particles, whereas the high energy resonance comes from the plasmon excitation perpendicular to the particle chain. The observation of both resonances in one spectrum became possible by using an angle of 70° with respect to the incident light, including both resonances. However, the two different resonances can be 'observed' with the naked eye: looking along the pores the membranes appear red, but blue perpendicular to the membrane surface. Fig. 8 illustrates the situation concerning the different colors and Fig. 9 shows gold colloid-filled membrane viewed along the long axes.

The particle size distribution can be reduced if preformed colloids are used instead of thermally generated ones. They can be transported into the pores by vacuum induction of solutions with subsequent drying. By this method, the filling

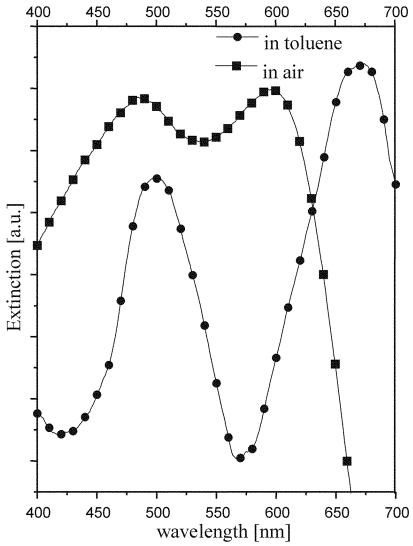

Fig. 7 Extinction spectra of gold nanoparticles/alumina composites in air and in toluene. The low energy plasmon resonances correspond to absorption along the long axis; the high energy peaks come from excitation perpendicular to the particle chain.[27]

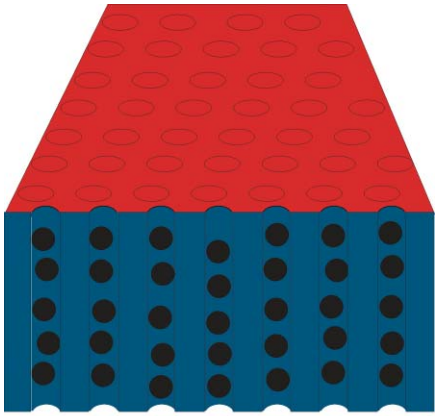

Fig. 8 Sketch of a gold particle-filled nanoporous membrane indicating the appearance of red and blue light.

grade can be varied by repeated filling. Less filled membranes show absorption maxima like those of corresponding isolated particles. Increasing concentrations broaden the resonances, ending up with two signals at higher and lower wavelengths, as discussed before.[27]

Simulations of the described experimental results agree quite well.[27,29,30]

Luminescent materials in alumina anopores

Photoluminescent silicon

Siloxenes are known as photoluminescent materials. Their composition can be described by the idealized formula $Si_6O_3H_6$. Three different structures have been proposed to exist.[31] They are shown in Fig. 10a–c.

Type 1 consists of silicon layers with only Si–Si bonds in the layer and with H atoms and OH groups to saturate free valences (Fig. 10a). This type shows a strong luminescence which is caused by the excitation of electrons *via* a direct band gap. The resulting photoluminescence is found at 2.4–2.5 eV (540–520 nm). In type 2 there exist Si–O–Si– interactions, and free valences are blocked by H atoms (Fig. 10b). The direct band gap is at 2.95 eV. Type 3 consists of Si_6-rings which are

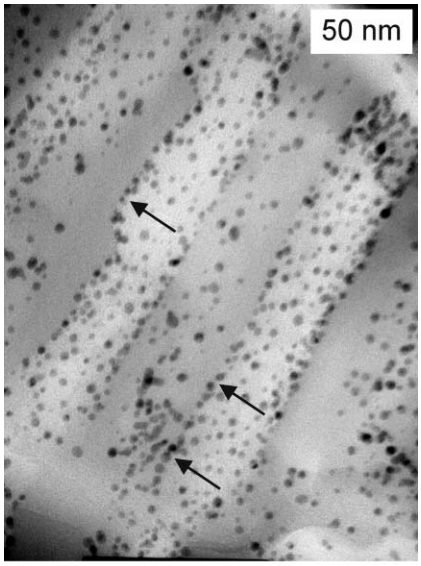

Fig. 9 TEM image of a sectioned alumina membrane with 4–5 nm gold particles. The arrows indicate short, wire-like assemblies of particles.

linked *via* O bridges and again with H atoms to saturate free valences (Fig. 10c). The band gap is 3.24 eV (380 nm).

The siloxene type 1 is probably formed in nanoporous alumina if pentamethylcyclopentadienyl silane, $C_5(CH_3)_5SiH_3$, is filled into the pores by vacuum induction and is then thermally decomposed at 800 °C in an atmosphere of nitrogen in the course of 5–10 min.[32] From IR investigation of such

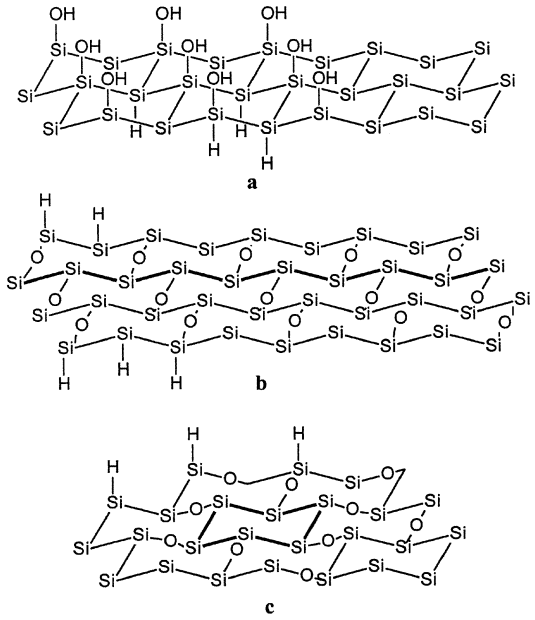

Fig. 10 Schemes of different siloxenes:[31] (a) type 1 with repeating Si_3OSiH and Si_3SiH moieties, (b) type 2 consisting of Si_2OSiH groups, and (c) type 3 built up also of Si_2OSiH groups with additional Si–Si bonds (Kautsky siloxene).

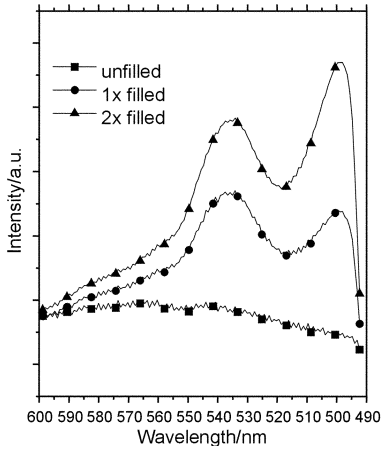

Fig. 11 Photoluminescence spectra of a 40 V alumina membrane unfilled, singly- and doubly-filled with silane and decomposed to siloxenes of type 1.

membranes it was concluded that the material inside the pores consists of siloxenes of type 1, since all typical frequences of this type could be observed. This was independent of the pore size.

The investigation of the luminescence properties of membranes with 20, 60, and 80 V pores showed two maxima, at 534–539 and 551–559 nm, respectively. Only 40 V membranes showed the signals at 494 and 530 nm. It should be mentioned that unfilled pores that have been fabricated in oxalic acid also show photoluminsecence in the same regions; however, this can be eliminated by thermal decomposition at 900 °C before filling. Repeated filling increases the signal intensities, as can be seen from Fig. 11 where typical spectra of an unfilled and a singly- and doubly-filled 40 V membrane are shown.

The signals at about 500 and 530 nm, corresponding with *ca.* 2.3–2.5 eV are in good agreement with the photoluminescence of siloxene type 1. We interpret the low energetic maxima by the existence of structure defects. They lead to an increase of the exciton binding energy and to the formation of electronic states in the band gap. Both processes decrease the photoluminescence energy. Of course, it cannot be excluded that repeated filling may also result in the formation of Si colloids.

Fig. 12 shows a sketch of a siloxene layer of type 1, fixed at the pore wall *via* strong Si–O–Al bonds, whereas Fig. 13 shows a piece of a siloxene-filled silica membrane under UV light.

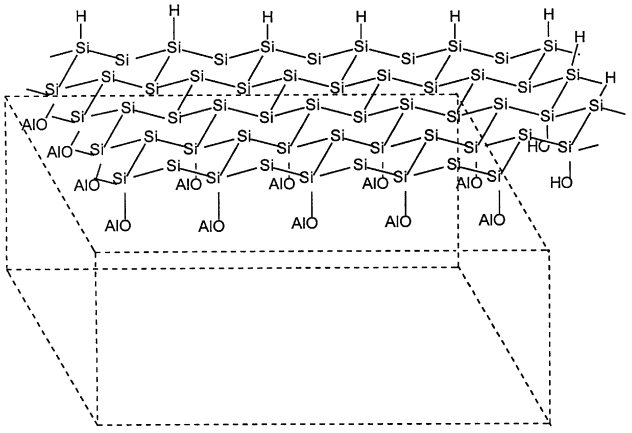

Fig. 12 Sketch of siloxene (type 1) on alumina pore wall.

Gallium nitride

Owing to its direct band gap of 3.45 eV[33] GaN is an interesting semiconductor for optoelectronic devices. Blue light emitting diodes (LEDs) or laser diodes (LDs) for the production of

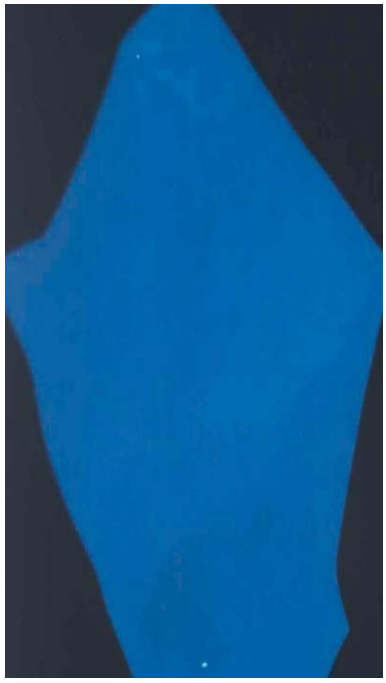

Fig. 13 Piece of a siloxene-filled alumina membrane under UV irradiation.[6]

novel displays and optical storage systems[34,35] are playing an increasing role in future technologies. For several years, numerous efforts have since been started worldwide to improve GaN technology. The optically transparent nanoporous alumina membranes might be considered as a novel approach for generating largely extended GaN arrays for several applications.[36]

In order to guarantee an optimized optical quality of the membranes, high quality aluminium must be used. Sulfuric acid as the electrolyte causes sulfur impurities of about 5% which, however, can be eliminated by heating up the membranes to 1000 °C for 1 h. Both the transparency as well as the pore structure are not influenced by this process. Membranes of *ca.* 200 μm thickness turned out to be the best with respect to mechanical stability.

The formation of GaN can in principle be achieved by the use of single source precursors.[37–40] The use of carbon-containing precursor molecules is disadvantageous for possible traces of carbon in the GaN which may quench luminescence. After a series of experiments with various single source precursors, we finally obtained our best results in generating GaN in the alumina pores by the reaction of Ga_2O_3 with NH_3 at 1000 °C in an atmosphere of nitrogen. The gallium oxide was first produced in the pores by thermolysis of $Ga(NO_3)_3$ which had been transported into the pores by means of an aqueous solution. After evaporating the water, the gallium nitrate was quantitatively decomposed to Ga_2O_3 at 1000 °C. Owing to the insolubility of Ga_2O_3 in water this process can be repeated as often as necessary. After Ga_2O_3 deposition, reaction with NH_3 at 1000 °C, diluted with a flow of nitrogen, gives crystalline nanoparticles of GaN. The formation of GaN can be shown by different methods. The ^{71}Ga NMR (91.53 MHz) signal at 340 ppm as well as the powder X-ray data agree fully with literature data.[41]Fig. 14 shows the X-ray diffractogram of a singly- and a fivefold-filled membrane. The increase of intensity and the decrease of the signal width clearly demonstrate the growth of the nanoparticles in the pores with repeated GaN formation processes.

Using the Scherrer formula, the average particle size can be calculated from the half width of the signals. The maximum particle size of 23.8 nm is reached after fivefold repeated filling and agrees well with the pore diameter of *ca.* 24 nm.

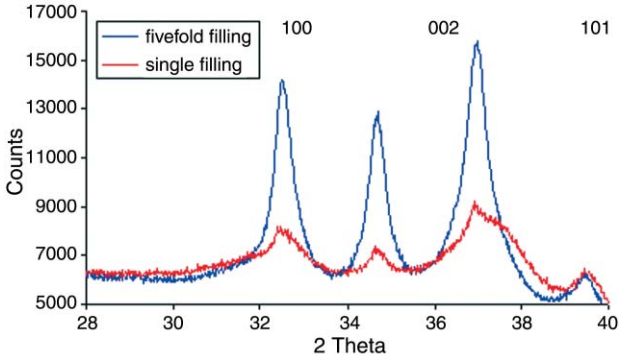

Fig. 14 XRD pattern of GaN in an alumina membrane after single (red) and fivefold (blue) filling.

Fifteen-, 20-, and 25-fold GaN formation did not result in any further change. Obviously, only the number of nanoparticles increases, and not their size. This is an impressive example for the size-limiting function of the porous material.

The photoluminescence spectra of as-prepared GaN/alumina hybrid systems show two signals, at 350 and 360 nm, corresponding to 3.54 and 3.44 eV. The 360 nm signal agrees with that of bulk GaN,[42] whereas the slightly higher energetic signal is caused by 2–3 nm GaN nanoparticles. As the intensity of the luminescence signals is rather low the spectra have only been recorded of four- and fivefold-filled membranes. They don't differ visibly.

Cadmium sulfide

Cadmium sulfide is another material that can be generated inside the nanopores whether from single source precursors or by reaction of two compounds. $CdCl_2$, $CdSO_4$ or $Cd(CH_3CO_2)_2$ can be used in aqueous solution to react with gaseous H_2S and to precipitate insoluble CdS. Formed HCl, H_2SO_4, and CH_3CO_2H can be removed together with water in vacuum. As-prepared CdS nanocomposites show the known orange photoluminescence.[6,43] A series of parameters such as concentration, H_2S contact time, thermal conditions, number of repetitions, and pore size influence the emission which is usually visible by a broad signal in the range of 600–750 nm (2.0–1.6 eV). An alternative procedure turned out to allow much more easily controlled reaction conditions. The known single source precursor $Cd(CH_3COS)_2(tmeda)$[44] can be transformed to CdS by two methods: reaction with H_2S at room temperature, or thermal decomposition at 125 °C. The cadmium thioacetate is transported into the pores as a 0.5 molar solution in dichloromethane. All components except CdS can be quantitatively removed in vacuum. EDX analyses indicate the existence of CdS in the pores. Fig. 15[45] shows a cutout of a CdS layer on the pore wall.

Fourier transformation of the electron diffraction pattern shows the lattice fringes of 0.34 nm of hexagonal CdS.

As-filled membranes exhibit photoluminescence between 550 and 800 nm (2.25–1.55 eV) with a maximum in the orange region.[45] In the case of using the H_2S decomposition method, there is an additional high energetic excitonic fluorescence between 460 and 500 nm (2.70–2.48 eV), depending on the experimental conditions, and is detected as a sharp emission band up to an excitation wavelength of 415 nm, as can be seen from Fig. 16.

Experiments to activate the fluorescence by doping with manganese failed in the case of wet chemically produced CdS membranes. However, in the case of the decomposition of $Cd(CH_3COS)_2(tmeda)$, doping experiments with manganese, but also with silver between 10^{-5} and 10 at%, increased the photoluminescence remarkably. Manganese was added as $Mn_2(CO)_{10}$, silver as Ag(COD)(hexafluoroacetylacetonate).[46]

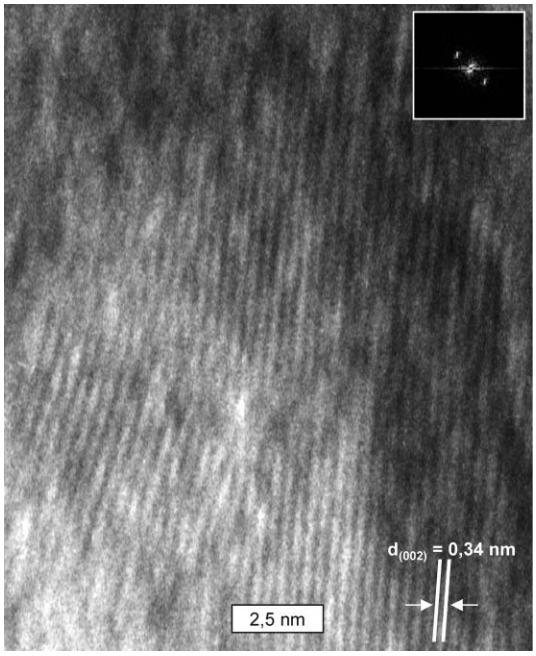

Fig. 15 Cutout of a CdS layer showing the lattice fringes of 0.34 nm in agreement with hexagonal CdS. Insert: Fourier transform of the lattice.

For instance, doping with 10^{-3} at% Mn causes an increase of intensity by a factor of 4, combined with a shift of the maximum from 610 nm (2.03 eV) to 551 nm (2.25 eV), compared with the undoped probe (Fig. 17).

0.1 at% of Ag gives the same increase of intensity.

Finally, Fig. 18 shows the TEM image of an ion-etched alumina membrane decorated with Ag-doped CdS nanoparticles. Series of modifications showed that the particle size correlates with the photoluminescence properties. Highest intensities were observed for particles <4 nm.

Concluding remarks

Nanoporous alumina turned out to be a unique material. This is due to its easy availability in any size and shape and, above all, its nature, based on the presence of 10^9–10^{11} pores per cm^2, running parallel through the optically transparent membranes

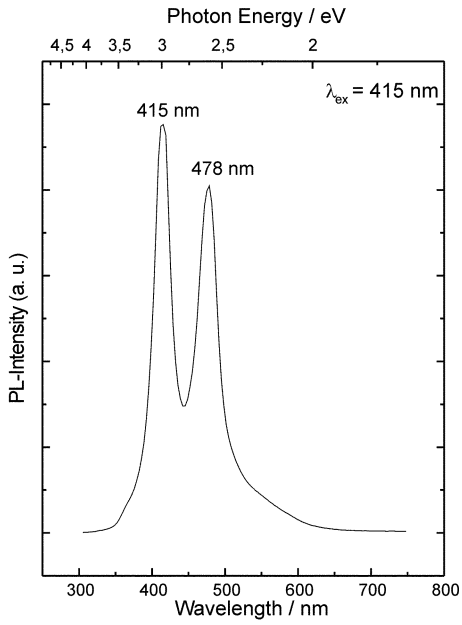

Fig. 16 Photoluminescence spectrum of a CdS-containing membrane, prepared by the H_2S decomposition method (see text).

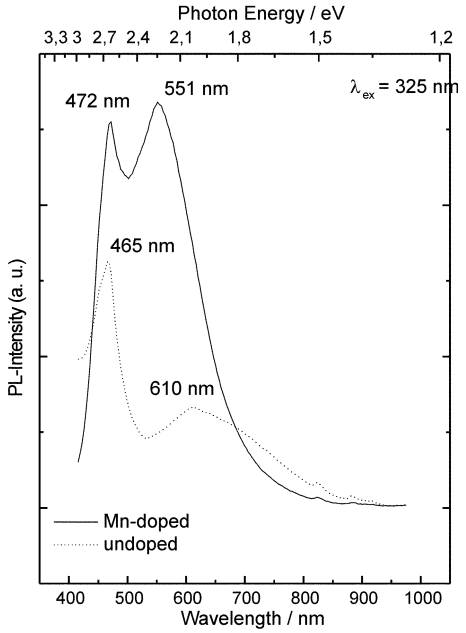

Fig. 17 Photoluminescence spectra of CdS in alumina membranes, made of $Cd(CH_3COS)_2$(tmeda). Dotted line: undoped membrane; solid line: doped with 10^{-3} at% Mn.

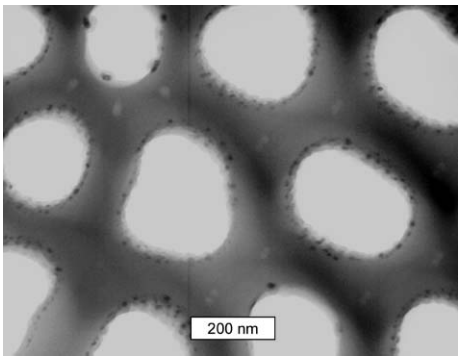

Fig. 18 TEM image of an ion-etched piece of alumina membrane. The walls are covered with CdS nanoparticles, doped with 0.1 at% Ag.

and adjustable in diameter in the range between 5 and 300 nm. The porous nature invites loading of the channels by different materials for many reasons. Materials with special optical, magnetic or electrical properties, positioned in the nanopores, must be nanostructured as well and so can transfer their size-dependent properties to the total membrane. The formation of metal nanowires inside the pores has frequently been practised for various reasons. In this article, the generation of magnetic Fe, Co, and Ni wires has been described and their magnetic properties discussed. The optical properties of gold nanoparticles in the pores have been studied with regard to the dependence of their size and orientation and have been compared with the results of simulations.

Photoluminescent layers of siloxenes could be prepared in the pores of alumina by thermolysis of $C_5(CH_3)_5SiH_3$. Gallium nitride nanoparticles were formed from Ga_2O_3 and NH_3 at 1000 °C, and finally, photoluminescent cadmium sulfide was generated in the pores from the single source precursor $Cd(CH_3COS)_2$(tmeda) by thermal decomposition or by reaction with H_2S. Doping of the CdS by manganese or silver increased the photoluminescence remarkably.

These various examples impressively demonstrate the versatility of nanoporous alumina membranes. No doubt that many other applications seem possible and several other groups have demonstrated that pores can indeed be used as useful nano reaction vessels.

A special kind of practical application of nanoporous alumina with important future relevance is its use in medicine. Medical implants can be coated with this kind of alumina, to act as fully biocompatible ceramics and, second, as a surface with enough space to store drugs or radionuclides to fabricate drug-loaded coronary stents and radioactive seeds. Local drug delivery systems have in addition been developed using the nanoporous films as adjustable membranes to deliver drugs over longer or shorter periods from a container. These applications have not been part of this feature article. The processes are described in several patents.[47–49]

Acknowledgements

The author would like to thank the coworkers who contributed to these results, M. Geerkens, I. Heim, Dr M. Kröll, Dr Y. Miquel, and Dr Th. Sawitowski. Furthermore he gratefully acknowledges financial supports from the European Committee (Brussels, TMR Network), the Deutsche Forschungsgemeinschaft and the Fonds der Chemischen Industrie (Frankfurt).

References

1 J. W. Diggle, T. C. Downie and C. W. Goulding, *Chem. Rev.*, 1969, **69**, 365.
2 J. P. O'Sullivan and G. C. Wood, *Proc. R. Soc. London*, 1970, **317**, 511.
3 G. E. Thompson and G. C. Wood, *Sci. Technol.*, 1983, **23**, 205.
4 M. M. Lohrengel, *Mater. Sci. Eng.*, 1993, **17**, 202.
5 G. E. Thompson, R. C. Furneaux, G. C. Wood, J. A. Richardson and J. S. Goode, *Nature*, 1978, **272**, 433.
6 G. Schmid, M. Bäumle, I. Heim, M. Kröll, F. Müller and T. Sawitowski, *J. Cluster Sci.*, 1999, **10**, 223.
7 A. Heilmann, F. Altmann, D. Katzer, F. Müller, T. Sawitowski and G. Schmid, *Appl. Surf. Sci.*, 1999, **144–145**, 682.
8 V. P. Menon and C. R. Martin, *Anal. Chem.*, 1995, **67**, 1920.
9 J. C. Hulteen and C. R. Martin, *J. Mater. Chem.*, 1997, **7**, 1075.
10 H. Masuda, K. Nishio and N. Baba, *Thin Solid Films*, 1993, **223**, 1.
11 T. Kyotani, L. Tsai and A. Tomita, *Chem. Commun.*, 1997, 701.
12 P. Mobery and R. C. McCarley, *J. Electrochem. Soc.*, 1997, **114**, L151.
13 D. Rontkevitch, A. A. Tager, J. Haruyama, D. AlMawlawi, M. Moskowits and J. M. Xu, *IEEE Trans. Electron. Devices*, 1996, **43**, 1646.
14 C. Schönenberger, B. M. I van der Zande, L. G. J. Fokkink, M. Henny, C. Schmid, M. Krüger, A. Bachtold, R. Huber, H. Birk and U. Staufer, *J. Phys. Chem. B.*, 1997, **101**, 5497.
15 D. G. W. Goad and M. Moskovits, *J. Appl. Phys.*, 1978, **49**, 2929.
16 P. Hoyer, *Adv. Mater.*, 1996, **8**, 857.
17 J. D. Klein, R. D. Herrick, D. Palmer, M. J. Sailor, C. J. Brumlik and C. R. Martin, *Chem. Mater.*, 1993, **5**, 902.
18 Y. G. Li and A. Lasia, *J. Electrochem. Soc.*, 1997, **144**, 1979.
19 T. Osaka, A. Kodera, T. Misato, T. Homma, Y. Okinaka and O. Yoshioka, *J. Electrochem. Soc.*, 1997, **144**, 3462.
20 S. Villain, P. Knauth and G. Schwitzgebel, *J. Phys. Chem. B.*, 1997, **101**, 7452.
21 J. Gruberger and E. Gileadi, *Electrochim. Acta*, 1986, **31**, 1531.
22 P. M. Paulus, F. Luis, M. Kröll, G. Schmid and L. J. de Jongh, *J. Magn. Magn. Mater.*, 2001, **224**, 180.
23 E. H. Frei, S. Shtrikman and D. Treves, *Phys. Rev.*, 1957, **106**, 446.
24 A. Aharaoni and S. Shtrikman, *Phys. Rev.*, 1958, **169**, 1522.
25 *Optical Properties of Metal Clusters*, U. Kreibig and M. Vollmer, ed., Springer, Berlin, 1995.
26 G. Mie, *Ann. Phys.*, 1908, **Z5**, 377.
27 T. Sawitowski, Y. Miquel, A. Heilmann and G. Schmid, *Adv. Funct. Mater.*, 2001, **11**, 435.
28 T. Castro, R. Reifenberger, E. Choi and R. P. Andres, *Phys. Rev. B.*, 1990, **13**, 8548.
29 D. Schönauer, M. Quinten and U. Kreibig, *Z. Phys. D.*, 1989, **12**, 527.
30 M. Quinten and U. Kreibig, *Appl. Opt.*, 1993, **32**, 6173.
31 L. Brus, *J. Phys. Chem.*, 1994, **98**, 3575.
32 A. Heilmann, P. Jutzi, A. Klipp, U. Kreibig, R. Neuendorf, T. Sawitowski and G. Schmid, *Adv. Mater.*, 1998, **10**, 398.
33 T. J. Goodwin, V. J. Leppert, C. A. Smith, S. H. Risbud,

M. Niemeyer, P. P. Power, H. W. Lee and L. W. Hrubesh, *Appl. Phys. Lett.*, 1996, **69**, 3230.
34 G. Fasol, *Science*, 1996, **272**, 1751.
35 Y. Yang, V. J. Leppert, S. H. Risbud, B. Twamly, P. P. Power and H. W. Lee, *Appl. Phys. Lett.*, 1999, **74**, 2262.
36 M. Geerkens, PhD thesis, University of Essen, 2002.
37 A. C. Frank and R. A. Fischer, *Adv. Mater.*, 1998, **10**, 961.
38 M. Niemeyer, T. J. Goodwin, S. H. Risbud and P. P. Power, *Chem. Mater.*, 1996, **8**, 2745.
39 C. M. Balhas and R. F. Davis, *J. Am. Ceram. Soc.*, 1996, **79**, 2309.
40 V. I. Ulyanov, *Phys. Status Solidi A.*, 1976, **34**, K195.
41 R. Juza and H. Hahn, *Z. Anorg. Chem.*, 1938, **239**, 282.
42 H. Winkler, A. Birkner, V. Hagen, I. Wolf, R. Schmeckel, H. v. Seggern and R. Fischer, *Adv. Mater.*, 1999, **11**, 1444.
43 H. Weller, *Angew. Chem.*, 1993, **105**, 43; H. Weller, *Angew. Chem., Int. Ed. Engl.*, 1993, **32**, 41.
44 M. Nyman, M. J. Hampden-Smith and E. N. Duesler, *Chem. Vap. Depos.*, 1996, **2**, 171.
45 I. Heim, PhD thesis, University of Essen, 2002.
46 G. Doyle, K. A. Eriksen and D. van Engen, *Organometallics*, 1985, **4**, 830.
47 Patent DE 19855421 C2, 2001.
48 Patent DE 19910188.4-45, 2001.
49 Patent DE 19948783 C2, 2001.